Comparison of low frequency seismic data to well logs - Hussar example

Heather J.E. Lloyd and Gary F. Margrave

ABSTRACT

Low-frequencies that are absent in seismic data impair accurate estimation of acoustic impedance. There are several methods for restoring these missing frequencies; they can be estimated by model inversion, borrowed from well logs, predicted using the available frequencies in the spectra, or recorded in the field. This paper uses the Hussar low-frequency experiment to investigate the low-frequencies available in the data recorded by three types of receivers and two of the four sources. The receivers used were 10Hz geophones, 4.5Hz geophones and Vectorseis MEM accelerometers. The sources used were 2 kg of dynamite at 15 m and a custom low-dwell sweep done by an INOVA 364 vibrator, a low frequency vibe. We compare stacked data, created with a flow that included Gabor decon, to the sonic and density logs in well 12-27. From each of 6 stacks, we constructed average traces at the well location by summing over a 230m wide spatial window centered on the well. To compare the different types of receivers to each other they were first correlated to match the accelerometer data and then the amplitude and phase were matched to the well reflectivity data for each source. A synthetic seismogram was created using the well logs and convolved with a zero phase low-pass wavelet designed to attenuate frequencies higher than 60Hz, this was then correlated with the accelerometer in time to accommodate any time shifts in the events. The low-frequency impedance trends were compared with the well impedance trends for the dynamite and INOVA low-dwell data. The 4.5Hz dynamite data had the best trend correlation with the well. BLIMP (Band-Limited IMPedance) inversions were done on both the dynamite and INOVA low-dwell data sets using low-frequency cut-offs of 1Hz and 5Hz. The INOVA low-dwell BLIMP inversions produced good inversions using a low cut-off of 3Hz for the accelerometer and 4.5Hz geophone receivers. Consistent BLIMP inversions were computed using a low-frequency cut-off of 1Hz for both the accelerometer dynamite data and the 4.5Hz dynamite data. These inversions matched the well and each other suggesting there could be consistent low-frequency information in recorded dynamite data as low as 1Hz.

INTRODUCTION

Field recorded data are generally bandlimited. The source does not emit a full band of frequencies and due to instrumentation limitations, the receivers do not record a full band of frequencies without distortion. Inverting the bandlimited data for impedance and rock properties creates a significant issue, as the trend of the impedance occurs mostly within the frequency band of 0-5Hz (Lindseth, 1979) where both sources and receivers are significantly challenged. Without the impedance trend the inversions are grossly inaccurate. Different methods are available for restoring these frequencies including prediction methods, model-based methods, using well logs to fill in the missing frequencies and possibly using a source and receiver pair that can record the low frequency band. This study analyzes the low frequency response of the data recorded in the Hussar low-frequency shoot and its ability to produce better inversions.

The data that is being used was obtained from the Hussar low–frequency shoot (Margave et al., 2011), located near Hussar, AB. The line, oriented SW to NE, had a total length of 4.5 km and well 12-27 was close to the line at the south end. Three types of receivers were used including a 10Hz 3-component geophone, a 4.5Hz acoustic geophone, and a Vectorseis MEMs accelerometer. The 10Hz geophones and the accelerometers were spaced at 10 meter intervals along the line where the 4.5Hz geophones were spaced every 20 meters. To test the source response for providing low frequencies four types of sources were used. The sources were all spaced at 20 meter intervals and included 2 kg dynamite charges at a depth of 15m, a low-dwell sweep by the INOVA 364 (a low frequency vibrator) a linear sweep by the INOVA 364 and a low-dwell sweep by a Failing model y2400 vibrator. Even though there are twelve unique data sets, this paper will only investigate six of them including all the receivers from the dynamite source and the low-dwell sweep from the INOVA 364.

Each data set was processed (Isaac and Margrave, 2011) using a basic flow including Gabor deconvolution. The accelerometer data was first integrated to convert to particle velocity. No filters were applied as it was desirable to keep the bandwidth of the data as broad as possible. The stacked section for the dynamite source as recorded by the accelerometers can be seen in Figure 1, the 10Hz data can be seen in Figure 2, and the 4.5Hz dynamite data can be seen in Figure 3.

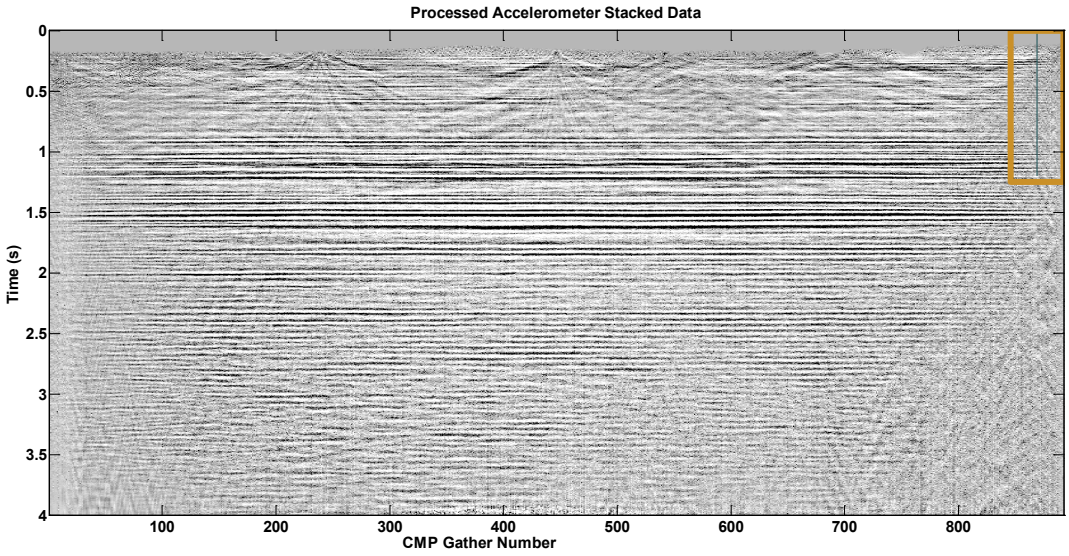

FIG 1: The integrated, processed accelerometer data from the dynamite shot. The well location is indicated in green and the traces used for this study are enclosed by the yellow box.

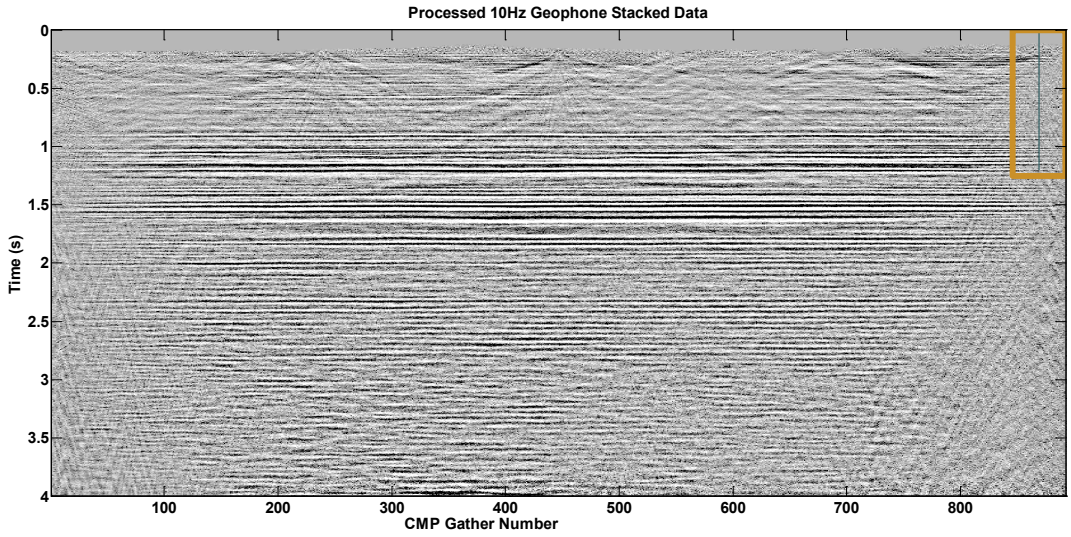

FIG 2: The processed 10Hz geophone data from the dynamite shot. The well location is indicated in green and the traces used for this study are enclosed by the yellow box.

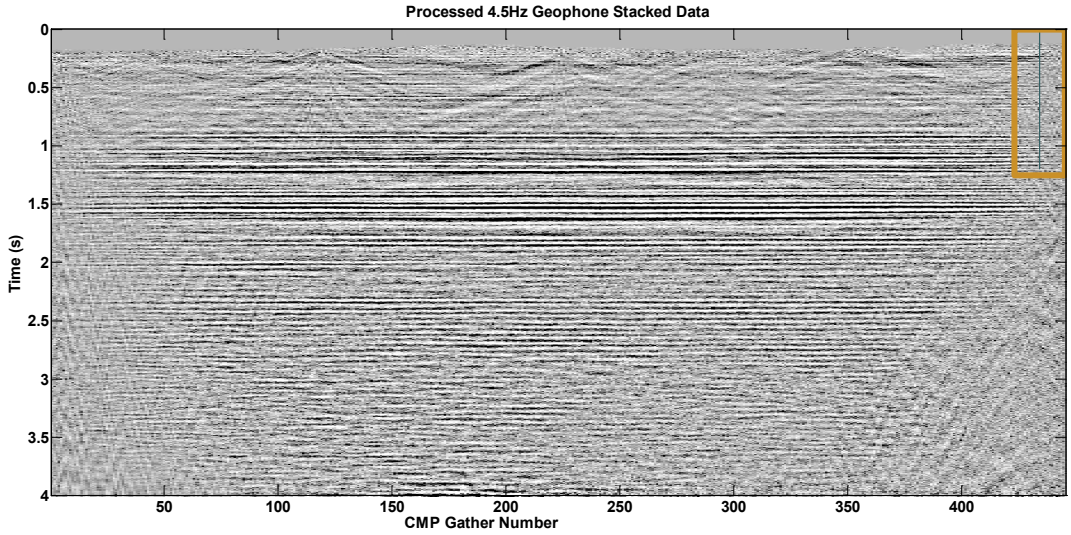

FIG 3: The processed 4.5Hz geophone data from the dynamite shot. The well location is indicated in green and the traces used for this study are enclosed by the yellow box.

METHOD

To compare the well to the seismic data, the well was projected onto the receiver line orthogonally. The nearest common midpoint (CMP) position was 869 (Figure 4). 23 CMP gathers on either side of 869 were averaged together to create the stacked trace used for analysis of the accelerometer data and the 10Hz geophone data. The gathers for the 4.5Hz data were spaced at twice the distance as the accelerometer and 10Hz data therefore only 11 CMP gathers on either side of the central trace were averaged. This way 230 m of CMP gathers were averaged at the central trace location, for all data sets.

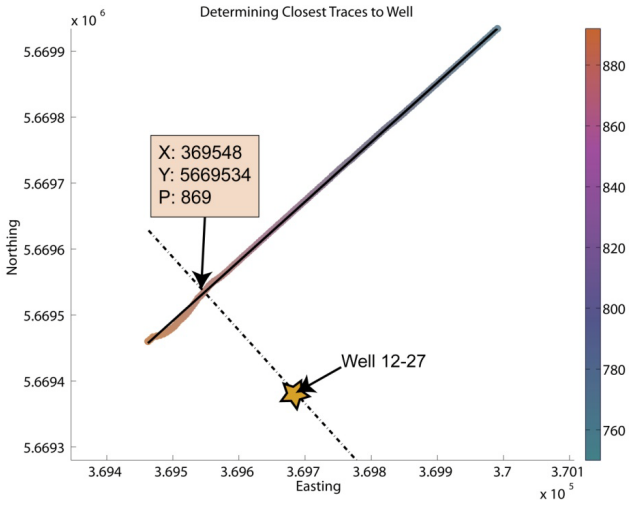

FIG 4: The receiver line is represented by the coloured dots which are coloured by the position or index. The black solid line represents the best fit line to the seismic receiver positions. The other line is orthogonal to the receiver line and projects the well onto the line. The closest receiver to the well is 869.

The 10Hz and 4.5Hz traces were correlated to the accelerometer data near the bottom of the well (0.75 – 1.05 seconds). To make the seismic data similar to the synthetic seismogram from the well, the amplitude spectra of the seismic data was smoothed with a 40Hz wide triangular smoother. The amplitude spectrum of the well reflectivity was also smoothed with the same smoother. The frequency spectrum of each dataset was then divided by its smoothed amplitude spectrum and multiplied by the smoothed reflectivity spectrum, Figure 5. The seismic data was analyzed by Isaac and Margrave (2011)and found to have a signal band that is mostly less than 60Hz for the dynamite source, therefore a [0 0 60 10] low pass filter was applied to the seismic data. A normal incidence synthetic seismogram with a zero phase [0 0 60 10] wavelet was created and is shown in Figure 6. To match the phase spectrum of the seismic data to the synthetic seismogram a least-squares constant-phase rotation was estimated and applied. A visual comparison of the synthetic trace and the stacked seismic traces can be seen in Figure 7. While the stacked traces matched the synthetic very well in the zone of interest, they did not match very well at earlier times. This suggests that a different phase rotation is required above the zone of interest. Figure 8, shows that estimated phase rotations do

vary in time and are similar for all dynamite stacked traces. For the purpose of this study the constant phase rotation calculated in the zone of interest was used. Once the traces were matched to the well reflectivity any response after 1.105 seconds was replaced with zeros.

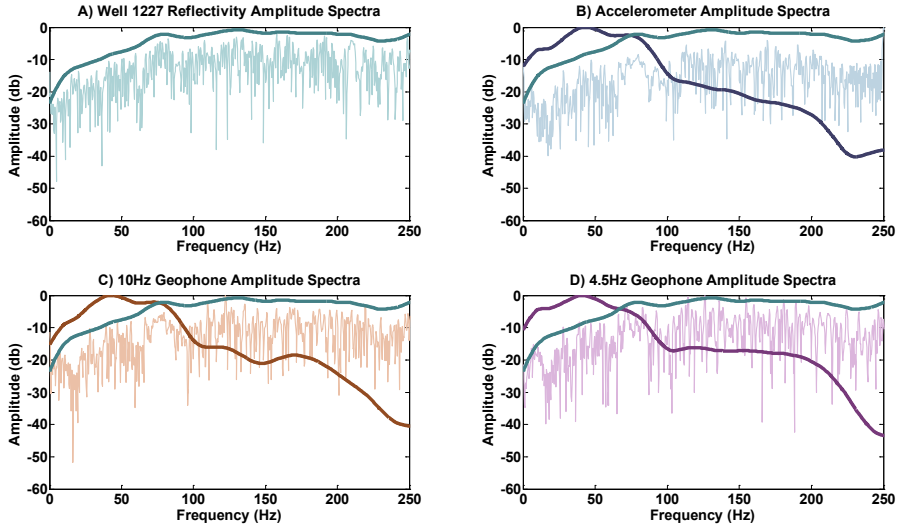

FIG 5: A) The amplitude spectrum of the well reflectivity (light teal) and the smoothed well reflectivity amplitude spectrum (teal). B) The corrected amplitude spectrum of the accelerometer stacked trace (light blue), the smoothed amplitude spectrum of the accelerometer stacked trace (blue) and the smoothed well reflectivity amplitude spectrum (teal). C) The corrected amplitude spectrum of the 10Hz stacked trace (light orange), the smoothed amplitude spectrum of the 10Hz stacked trace (orange) and the smoothed well reflectivity amplitude spectrum (teal). D) The corrected amplitude spectrum of the 4.5Hz stacked trace (light pink), the smoothed amplitude spectrum of the 4.5Hz stacked trace (pink) and the smoothed well reflectivity amplitude spectrum (teal).

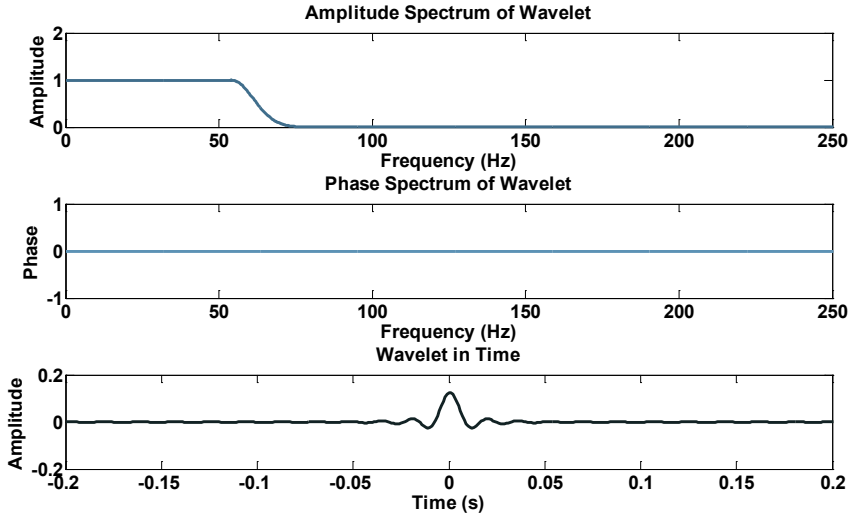

FIG 6: The wavelet used to construct the synthetic seismogram from well 12-27.

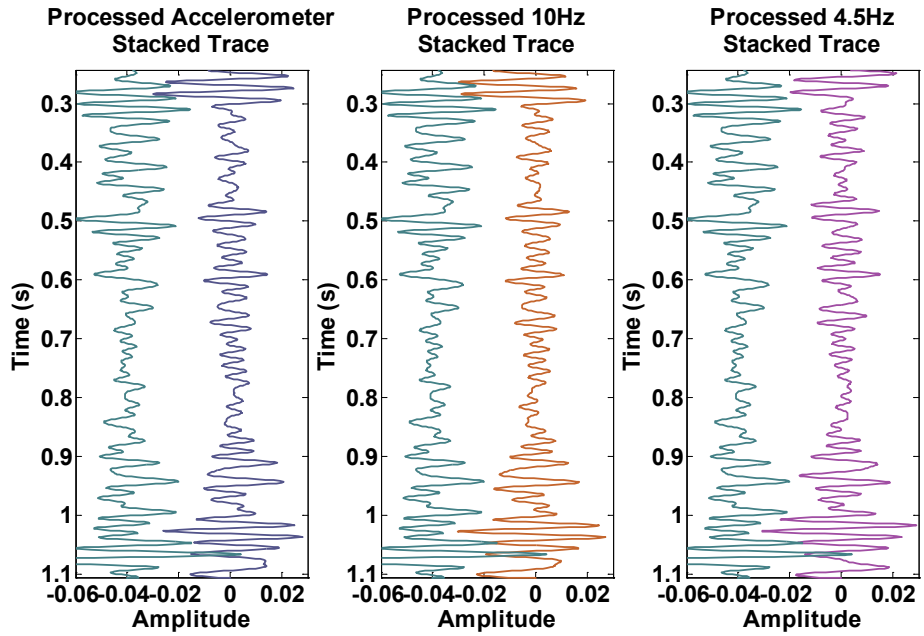

FIG 7: The well synthetic seismogram (teal) is compared with the different stacked traces.

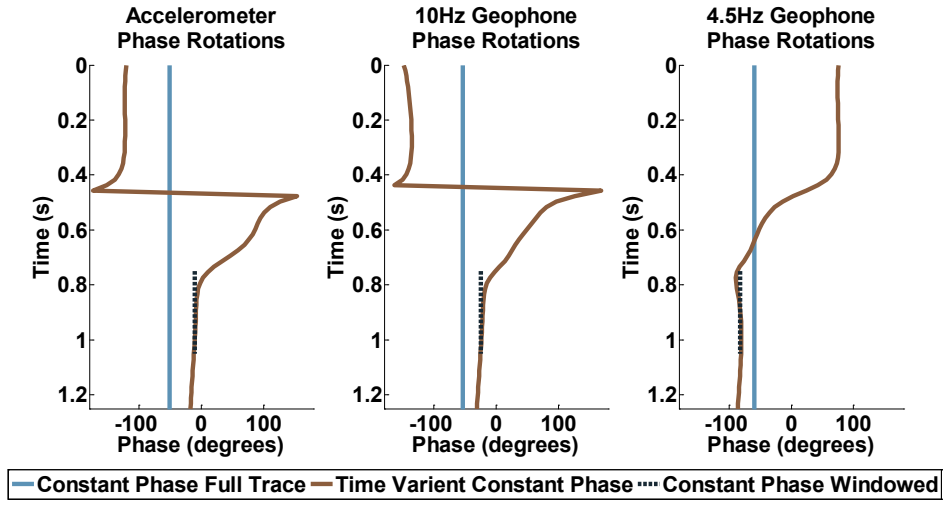

FIG 8: Dynamite phase rotations.

RESULTS

Dynamite Source

If we invert the dynamite traces for impedance using the standard recursion formula,

$$I_{j+1} = I_j \frac{1+r_j}{1-r_j} = I_0 \prod_{k=1}^{j} \frac{1+r_k}{1-r_k}, \quad (1)$$

where I_o is the impedance at the surface (e.g. Oldenburg et al., 1983), we get interesting results. For this example as the overburden is estimated we have started the recursion

formula at 0.243 seconds. Normally, with impedance inversion when the low frequency trend is missing from the reflectivity, the resulting impedance fluctuates around the I_o value. Figure 9 shows the impedance results for the dynamite data. The accelerometer inversion has a reasonable trend but it becomes unrealistic after about 0.6s while individual fluctuations between 0.4-0.6 seconds do reasonably match the well impedance. This indicates that the accelerometer data does have useable low frequencies but the very low frequencies are drowned out by the 1/frequency noise that is a common problem with accelerometers (Margrave et all, 2011). The 10 Hz inversion does show an impedance estimate that fluctuates around the I_o value. The 4.5Hz inversion shows a low-frequency trend that is very similar to the well impedance but diverges from the well impedance after about 0.75 seconds. This suggests that the 4.5Hz data has more useable low frequencies than the accelerometer data but is still missing reliable information in the very low-frequencies.

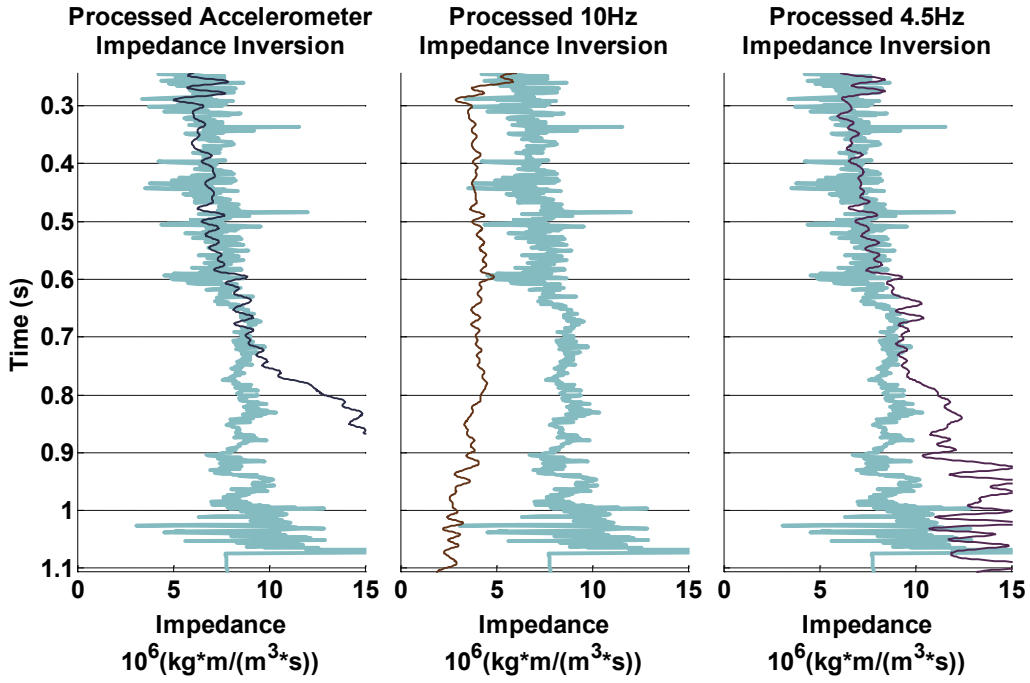

FIG 9: Recursion impedance inversions for the accelerometer data 10Hz geophone data and 4.5Hz geophone data. The well impedance is shown in teal. For better accuracy, the inversions start at the top of the recorded well impedance (0.243 seconds).

The amplitude spectra of the well impedance and inverted impedance were plotted together in Figure 10. The well impedance, needed to be scaled by a factor to compare it to the inverted impedance. The factor was determined by least squares between 2 and 20 Hz. This plot shows that the accelerometer, 10Hz geophone and 4.5Hz geophone impedance amplitude spectra are very similar from 5 to 20 Hz. The filtered well impedance from 0 to 1 Hz (Figure 11) has a similar trend as the filtered accelerometer and 4.5Hz inverted impedance till 0.75 seconds. For the filter panels of 1 to 2Hz and 2 to 3Hz, the 10Hz inverted impedance in not similar to the filtered well or other receivers. The accelerometer and 4.5Hz inverted impedance are very similar to each other but are not similar to the well impedance.

To determine if there is any similarity between the reflectivity of the well and the stacked traces the amplitude spectra were compared, Figure 12. The amplitude spectrum of the receivers tends to be similar to each other from 5Hz to 20Hz. The accelerometer and 4.5Hz geophone spectra are similar from below 2Hz as well. No receivers appear to match at all with the well reflectivity spectra. This dissimilarity in the spectra may indicate that there is noise in the data that is not in the well log.

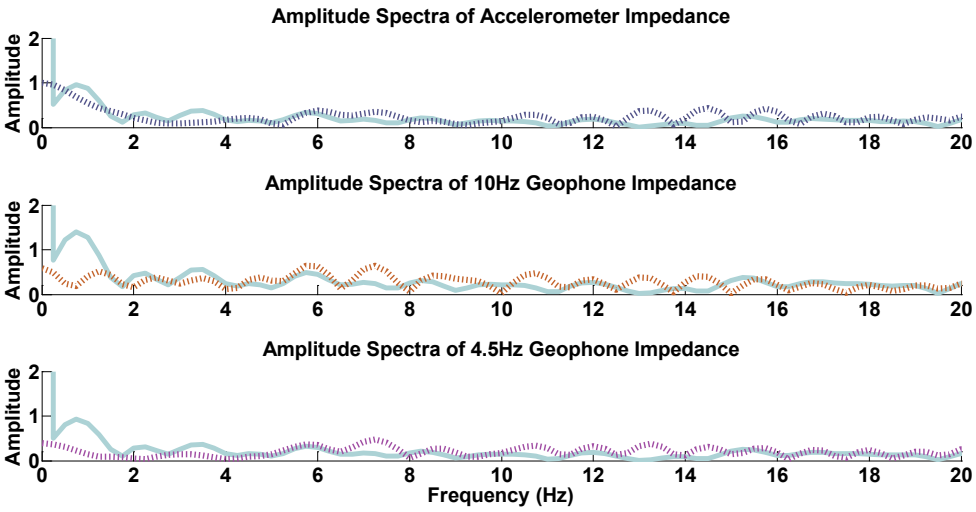

FIG 10: Amplitude spectra of accelerometer inverted impedance (blue), 10Hz geophone inverted impedance (orange), 4.5Hz geophone inverted impedance (pink) and scaled well impedance (light teal).

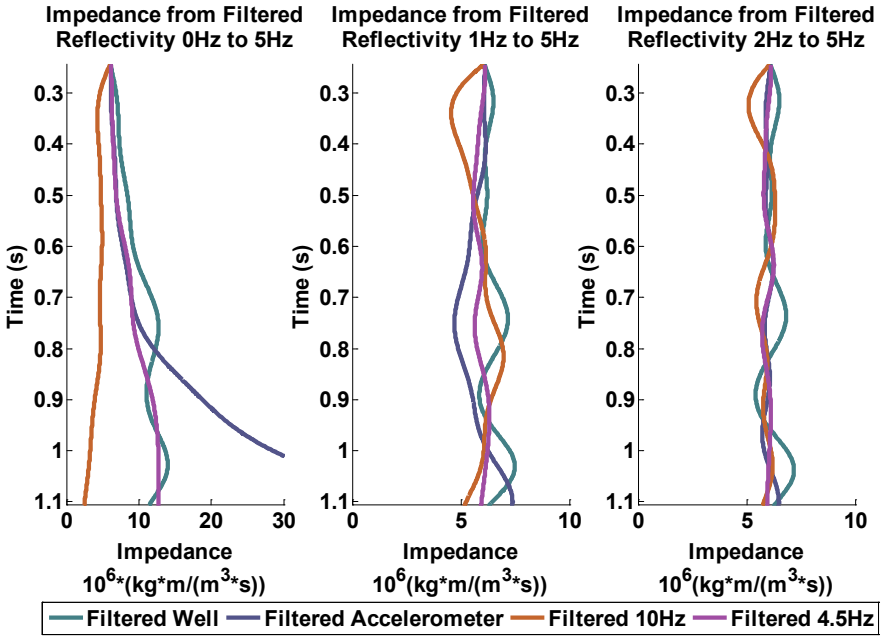

FIG 11: Filtered well impedance (teal), accelerometer inverted impedance (blue), 10Hz geophone inverted impedance (orange) and 4.5Hz geophone inverted impedance (pink) using different frequency bands.

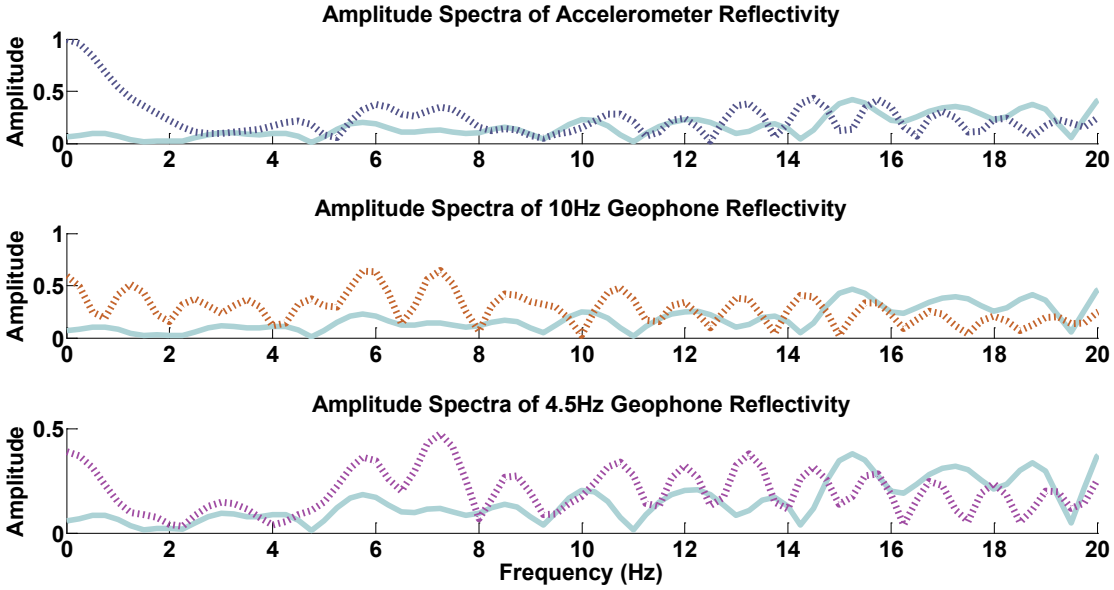

FIG 12: Amplitude spectra for well reflectivity (light teal), accelerometer stacked trace (blue), 10Hz geophone stacked trace (orange) and 4.5Hz geophone stacked trace (pink).

INOVA Low-Dwell Source

The INOVA low-dwell was prepared similarly to the dynamite data. 230m of CMP gathers were averaged to produce the stacked trace for each receiver. The different receivers were then correlated to match the accelerometer data. The frequency spectra of the receivers then normalized to the well reflectivity and then a [0 0 60 10] zero-phase low-pass filter was applied. The high portion of the signal band for the INOVA low-dwell source was indicated to be only 40Hz (Isaac and Margrave, 2011) but to keep continuity with the dynamite data the 60Hz filter was still applied. The corrected trace can be seen in Figure 13.

Using the recursion formula, the stacked traces were inverted for impedance and compared to the well impedance, these impedances were also calculated starting at the top of the recorded well (0.275 seconds). Figure 14 shows that the accelerometer data matches the well impedance until 0.65 seconds from which it then diverges. The 4.5Hz geophone inversion also follows the well trend to about 0.7 seconds, and then diverges. This suggests that the accelerometer and 4.5Hz geophone data contain some reliable low-frequency data, where the 10Hz data does not. Figure 15 shows the impedance amplitude spectra for the receivers and the well. The impedance amplitude spectra for the accelerometer and 4.5Hz geophone are very similar but are dissimilar to the well impedance. The amplitude spectra for the reflectivity are shown in Figure 16. The 4.5Hz reflectivity has a similar trend to the accelerometer data but is dissimilar from the well reflectivity. The 10Hz reflectivity does not have any similarity to the well. This is curious as the signal band of the INOVA low-dwell data is between 10Hz and 40Hz (Isaac and Margrave, 2011) so we should see some correlation of the spectra after 10Hz.

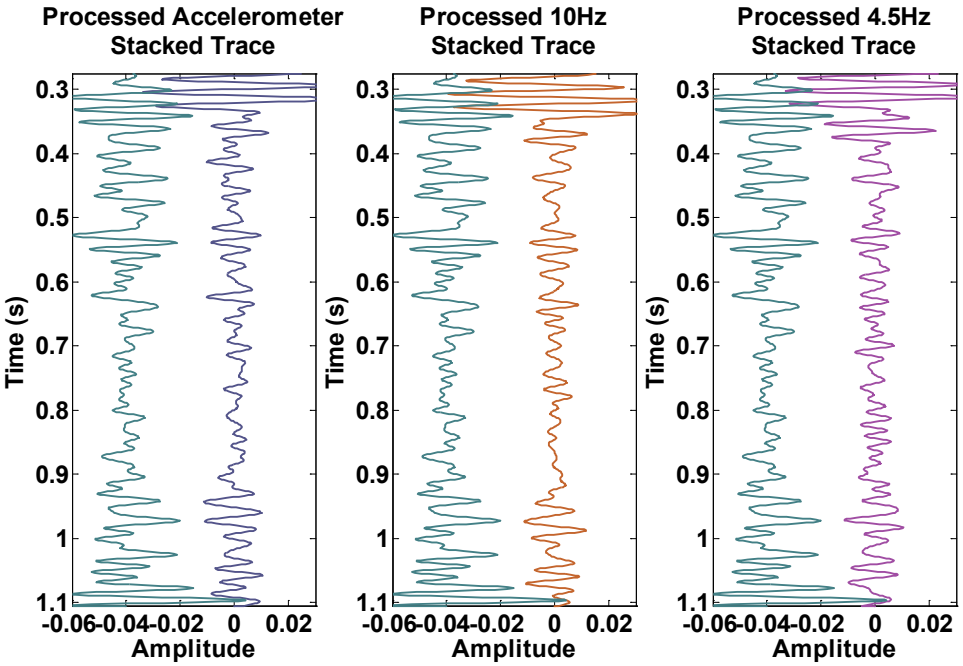

FIG 13: Correlated stacked traces compared with the well reflectivity (teal).

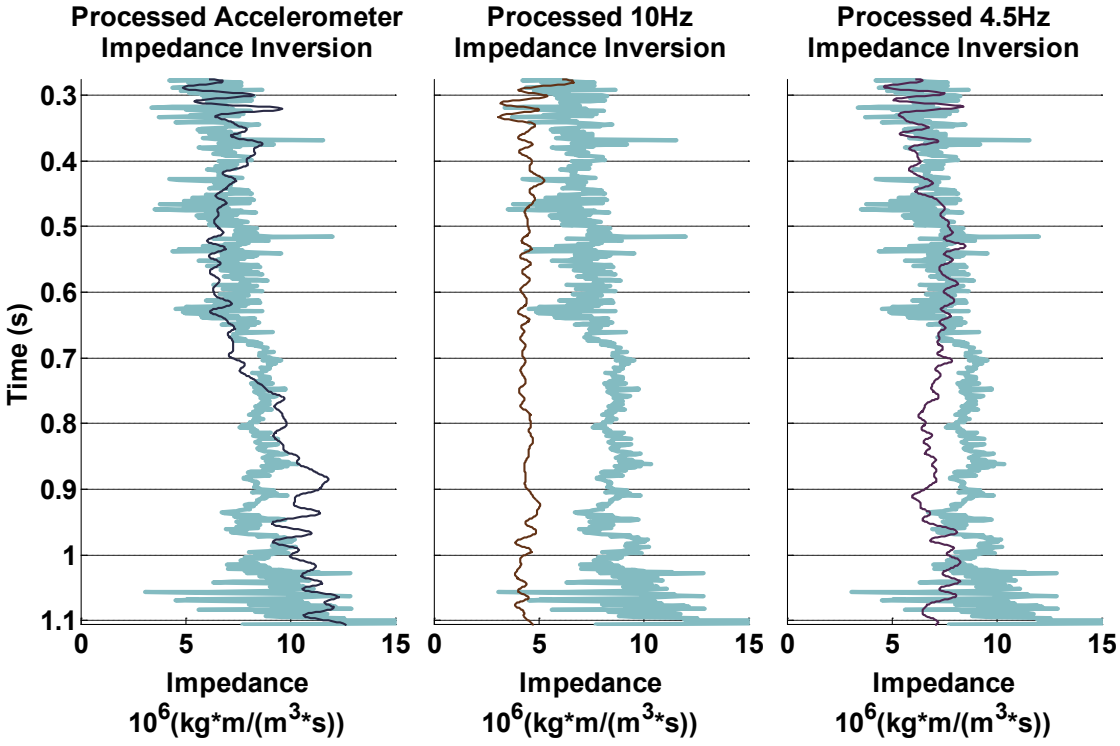

FIG 14: Recursion formula inverted impedance for accelerometer data 10Hz geophone data, 4.5Hz geophone data and scaled well impedance (teal).

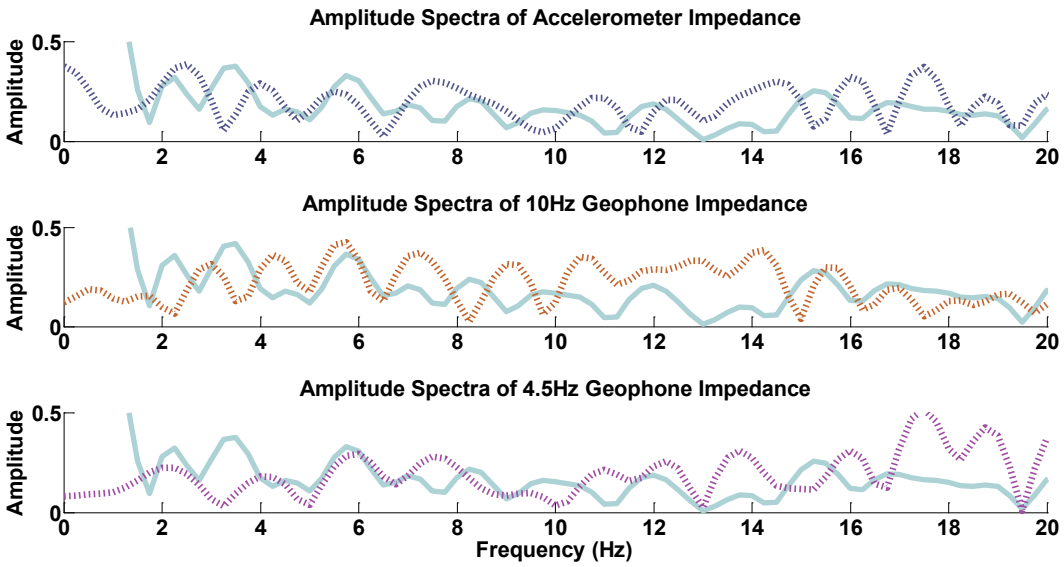

FIG 15: Amplitude spectra of accelerometer inverted impedance (blue), 10Hz geophone inverted impedance (orange), 4.5Hz geophone inverted impedance (pink) and scaled well impedance (light teal).

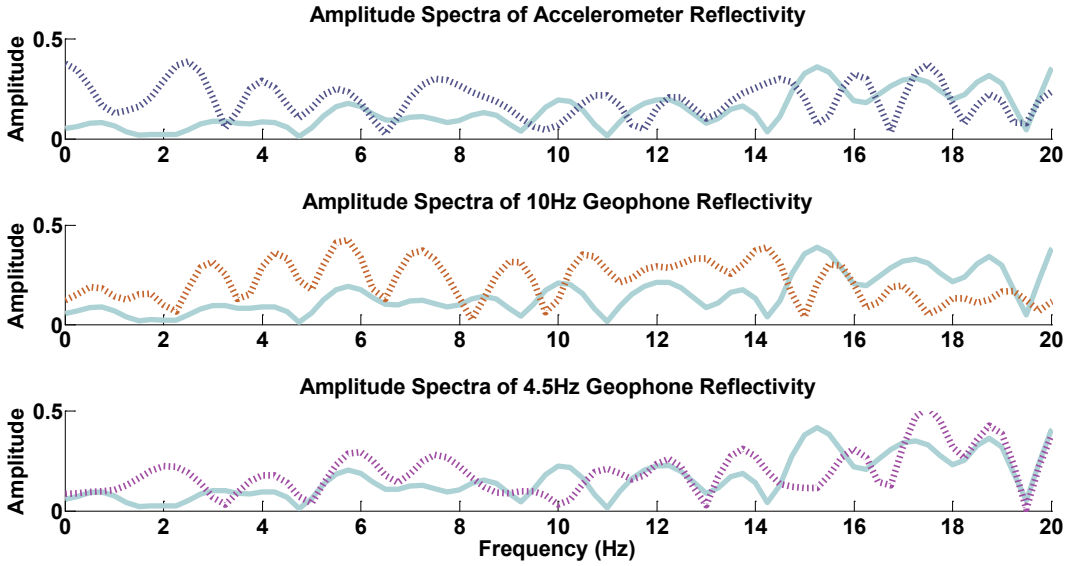

FIG 16: spectra for well reflectivity (light teal), accelerometer stacked trace (blue), 10Hz geophone stacked trace (orange) and 4.5Hz geophone stacked trace (pink).

Results have indicated that useful low-frequencies could be present in the 4.5Hz and accelerometer data. The effect of adding 0.5 to 2Hz of frequency information from the well log, instead of >5Hz which is normally used (Lloyd and Margrave, 2011), to the stacked traces, was tested using BLIMP (BandLimited Impedance inversion) experiment.

BLIMP Experiment

BLIMP is a method for borrowing the low-frequency data from wells and then using it to fill in missing frequencies in the data (Ferguson and Margrave, 1996). The goal of BLIMP is to use the minimal amount of log information so that the seismic data has more influence on the inversion and fill the low-frequency gap. When experimenting with different low frequency cut-offs (the frequency at which we stop borrowing the frequencies from the well log) we found that reasonable inversions could be made with only minimal (1Hz) frequency contribution from the well. This was suspicious as the low frequency content in the data was not trusted below 4Hz (Isaac and Margrave, 2011). To test the effect of inverting data that has a partially filled frequency spectrum, the following experiment was done.

To create a suitable model we needed to have lots of low frequencies that were attenuated so a zero-phase [10 20 60 80] Ormsby wavelet was chosen (Figure 17). This wavelet was then convolved with Well 12-27 to create a synthetic seismogram. To quantify the quality of the inversions, the well reflectivity was filtered by a low pass filter of [0 0 60 20] to remove the high frequencies and inverted using the recursion formula, Equation 1, this is referred to as the best possible impedance inversion (BPII). The BLIMP method works in the frequency domain by inverting the seismic data, filtering it and then adding the low frequencies from the well log and then calculating the inverse Fourier transform to get the result back in time, (Ferguson and Margrave, 1996). This method was repeated using various low-frequency cut-offs, Figure 18. Once this was completed, the reflectivity amplitude spectrum was examined and found that reasonable results were obtained even when there was a very large gap of missing frequencies from the cut off value to about 12Hz (Figure 19). The least squares error was calculated between the BLIMP inversions and the BPII, these results can be seen in Table 1. From this table we can see that even having a slight amount of low frequencies from the well increases the accurateness of the inversion significantly.

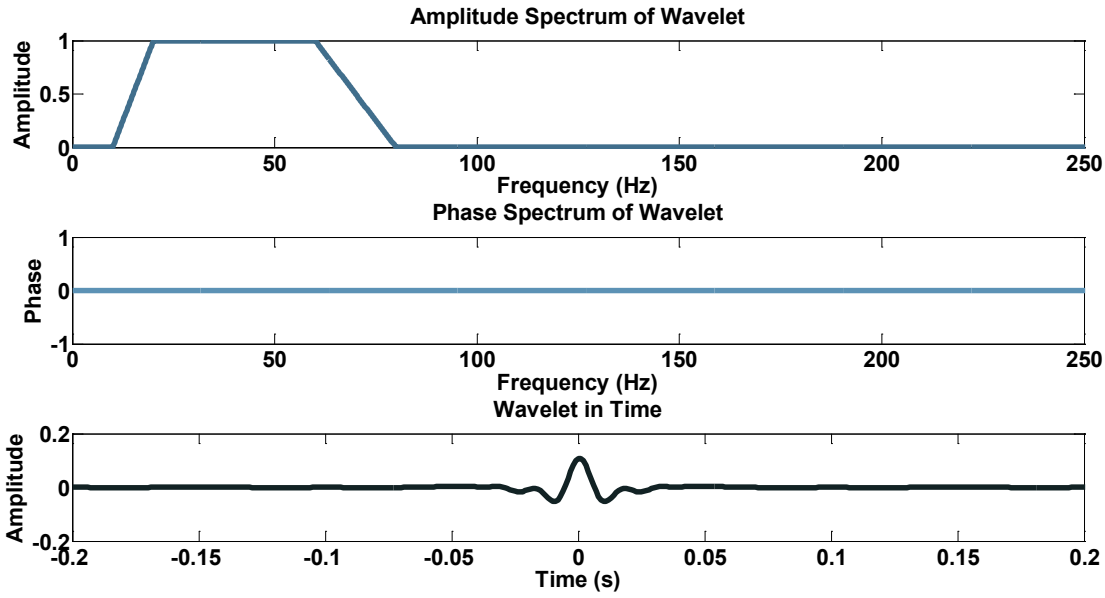

FIG 17: The wavelet used in the BLIMP experiment to create the well synthetic seismogram

Table 1: Least squares error between the best possible impedance inversion and BLIMP inversion results for various low-frequency cut-offs. The noisy synthetic trace had 0.5 signal to noise ratio, and the noise was only present in frequencies less than 15Hz.

Low Frequency Cut-Off	Synthetic BLIMP Error	Noisy Synthetic BLIMP Error	Low Frequency Cut -Off	Synthetic BLIMP Error	Noisy Synthetic BLIMP Error
0	149.52	92.80	5	15.30	19.56
0.5	27.51	26.95	6	13.74	17.83
1	25.98	25.38	8	12.43	16.90
1.5	22.93	22.56	10	10.55	13.30
2	21.24	22.23	12	9.20	12.51
2.5	18.10	20.95	14	9.06	10.52
3	17.74	20.37	15	8.56	8.54
3.5	16.29	20.41	16	8.31	8.29
4	15.99	19.95	18	7.91	7.89
4.5	15.99	19.37	20	7.80	7.80

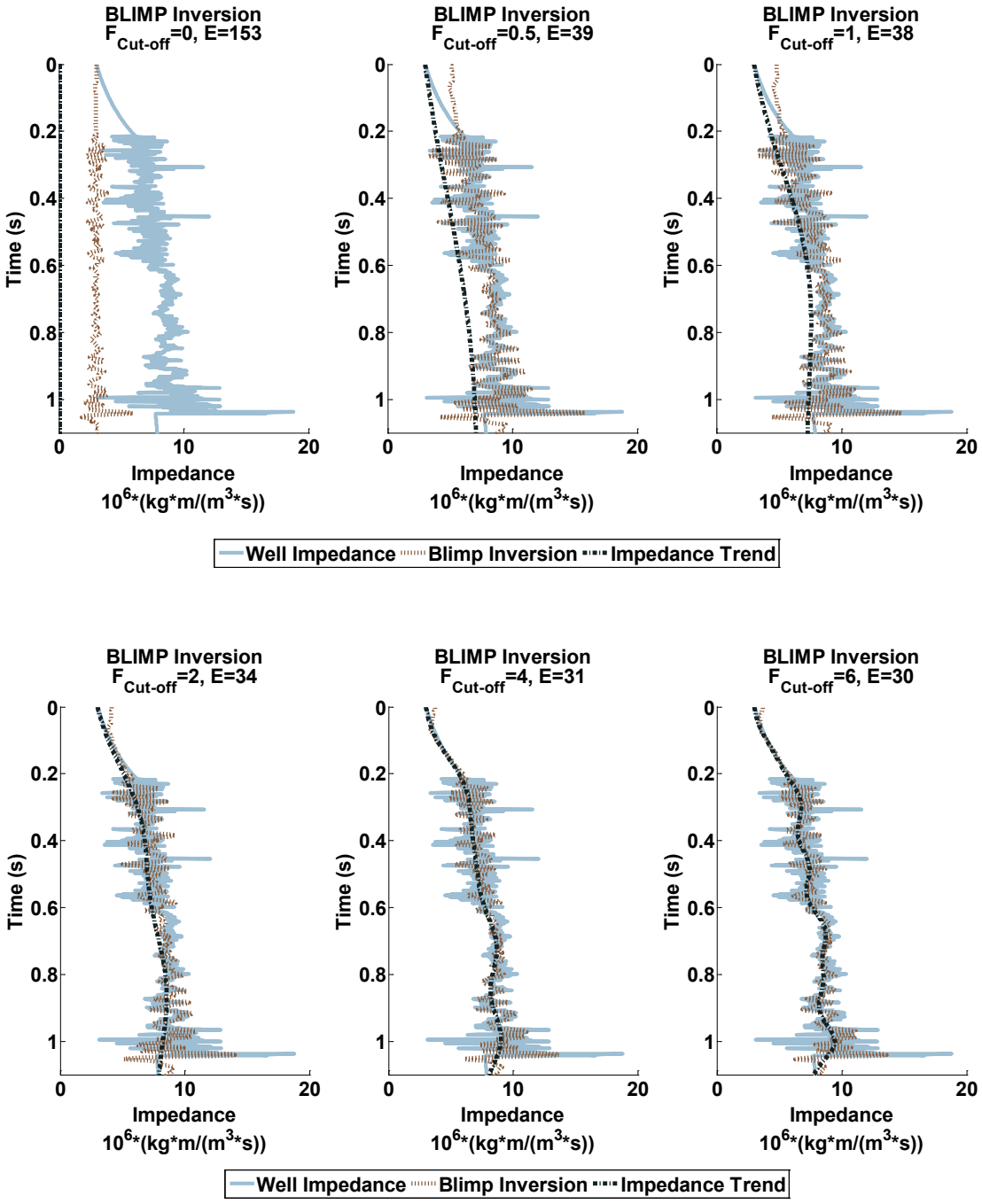

FIG 18: The BLIMP inversion results with various low-frequency cut-offs. The least squares error was calculated between the blimp inversion and the true well impedance. The error between the true well impedance log and best possible impedance inversion is 26.

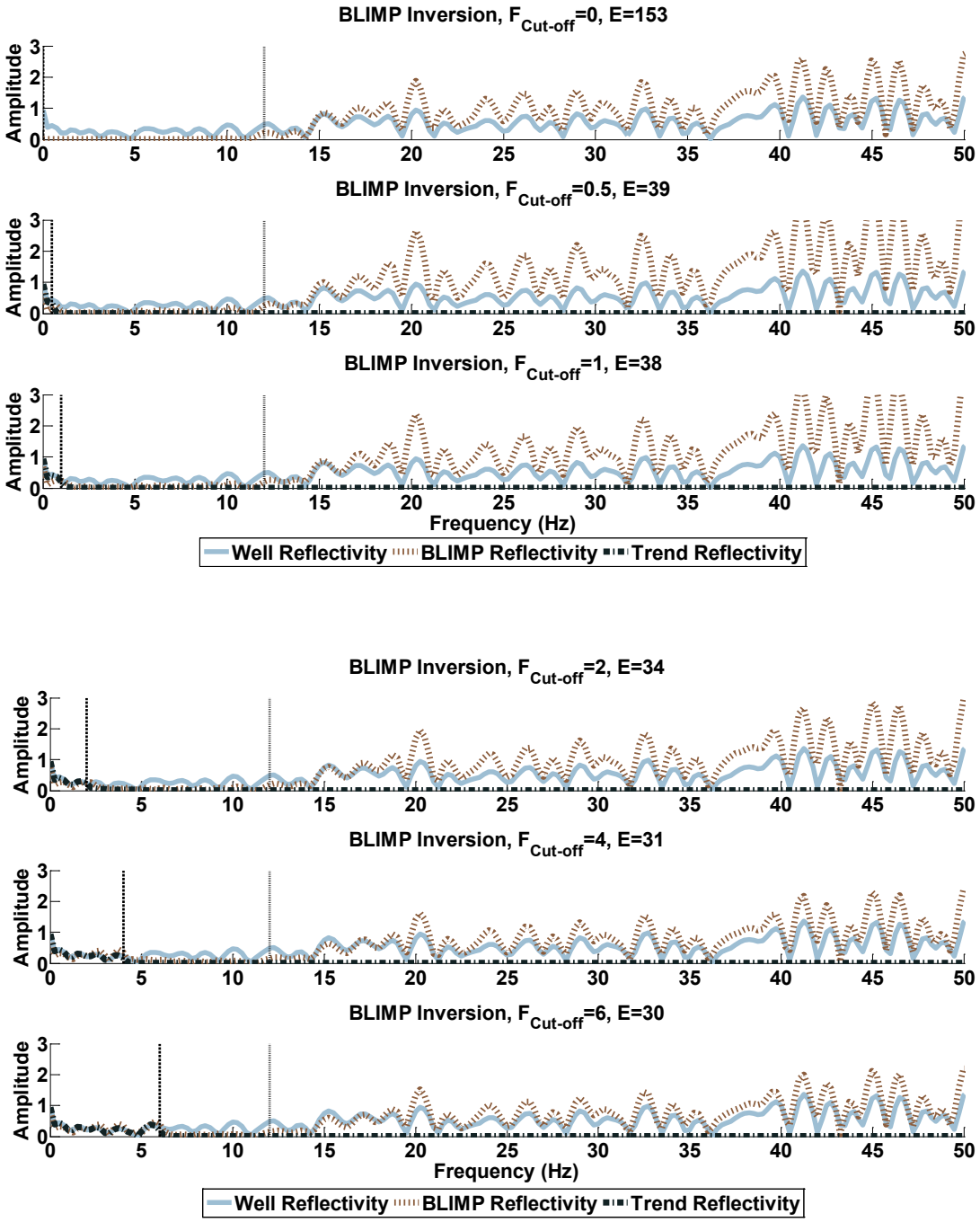

FIG 19: The amplitude spectra of the BLIMP inversion results with various low-frequency cut-offs. The least squares error was calculated between the blimp inversion and the true well impedance. The error between the true well impedance log and best possible impedance inversion is 26. The dashed black line represents the low-frequency cut-off and the black dotted line represents the end of the flat spectrum.

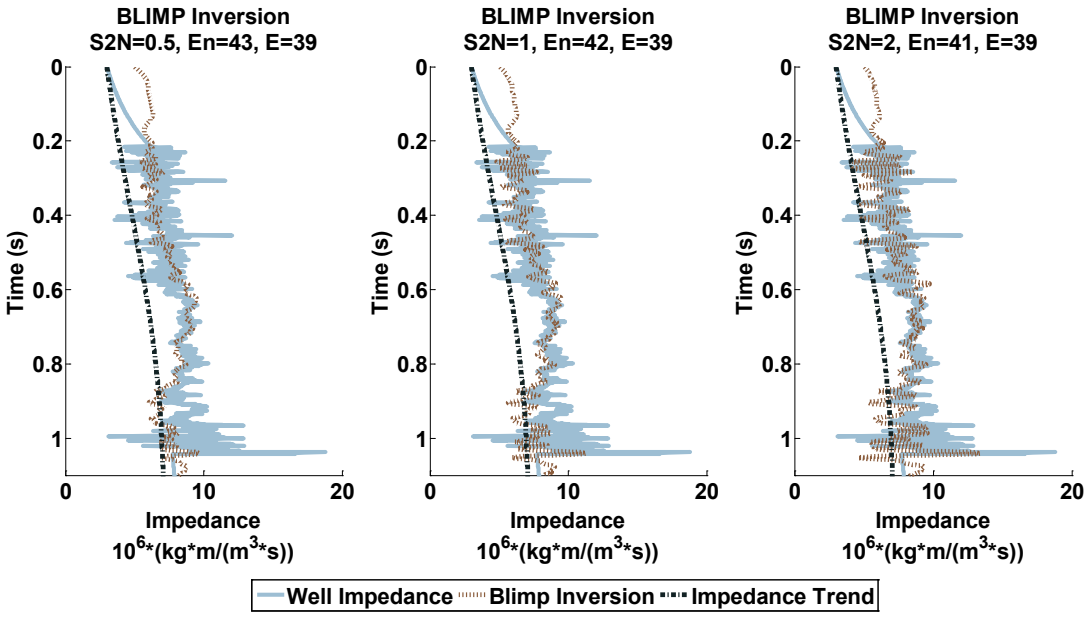

FIG 20: BLIMP impedance inversion on data with varying amounts of noise. The low-frequency cut-off value was 0.5Hz. E represents the error on a non-noisy data set with the same cut-off value. En is the least squares error between the true well impedance and the BLIMP inversion.

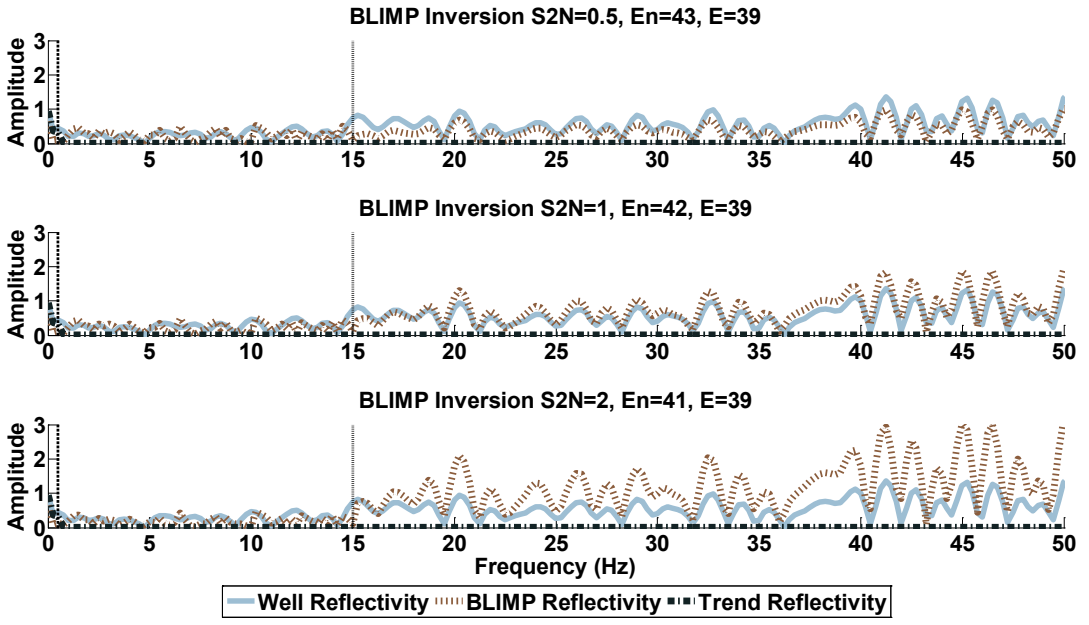

FIG 21 : The amplitude spectra of the BLIMP inversion results on data with varying amounts of noise. The low-frequency cut-off value was 0.5Hz. E represents the error on a non-noisy data set with the same cut-off value. En is the least squares error between the true well impedance and the BLIMP inversion. The error between the true well impedance log and best possible impedance inversion is 26. The dashed black line represents the low-frequency cut-off and the black dotted line represents the end of the noisy spectrum.

A flat spectrum in real data is rarely seen as noise is usually present in our data. To test if noise makes a difference when it is present in the low frequency gap, it was added in the frequencies from 0 to 15Hz. Several signal to noise ratios were tested and it was found that the noise did affect the inversions for all signal to noise values, Figure 20. The amplitude spectra for these inversion results can be seen in Figure 22. The most substantial differences were seen in the signal to noise values less than 1.Table 1 shows the error associated with inverting the data at different cut-offs when the signal to noise ratio is 0.5.

From this we can conclude that a missing gap in the spectrum does not affect the inversion substantially if there are zeros in the gap. If the data has a small signal to noise ratio, the noise can highly affect the impedance inversion.

BLIMP Inversions on Dynamite

BLIMP inversions were done on the dynamite data for low-frequency cut-offs of 1Hz and 5Hz. The 1Hz BLIMP inversion results (Figure 22) were very similar between the accelerometer data and the 4.5Hz geophone. The 4.5Hz inversion did follow the well more often and had slightly less error than the accelerometer inversion. The 10Hz geophone data followed the well impedance trend closely and did not vary much from it. Figure 23, shows the amplitude spectra for these inversions. The frequency content for all receiver types is very similar for frequencies of 20Hz and above. The accelerometer impedance spectra and the 4.5Hz spectra have a similar trend that is scaled when compared to one another at frequencies below 10Hz.

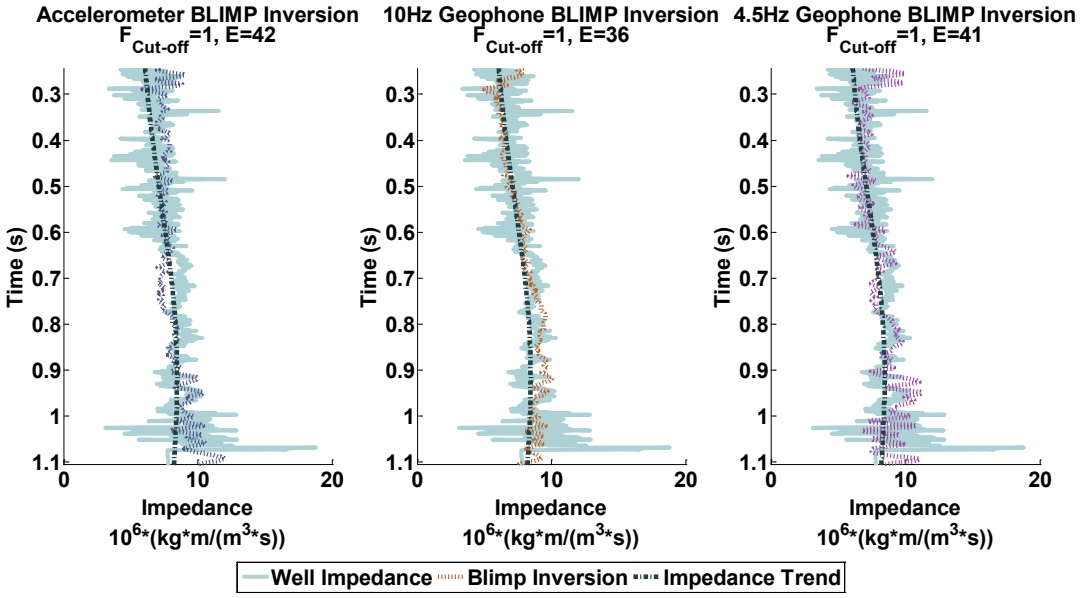

FIG 22: Impedance BLIMP inversions using a low-frequency cut-off of 1HZ. The least squares error (E) was calculated between the well impedance log and the BLIMP inverted impedance.

Another BLIMP inversion was done using a low-frequency cut-off of 5Hz, Figure 24. In these inversions all the results look very similar and follow the trend of the log. Figure 25 shows the amplitude spectra of the data. All the data sets have similar frequency spectra for frequencies higher than 20Hz; also the accelerometer data look very similar to

each other from 5 to 10Hz, as before. This result does not feel like it is optimum as the well log trend is fitting the data and there appears to be a large correlation between the low frequencies of the accelerometer data and the 4.5Hz. This could be evidence that low frequencies do exist in the dynamite data and we can satisfactorily use a low-frequency cut-off such as 1Hz to get a valid impedance inversion.

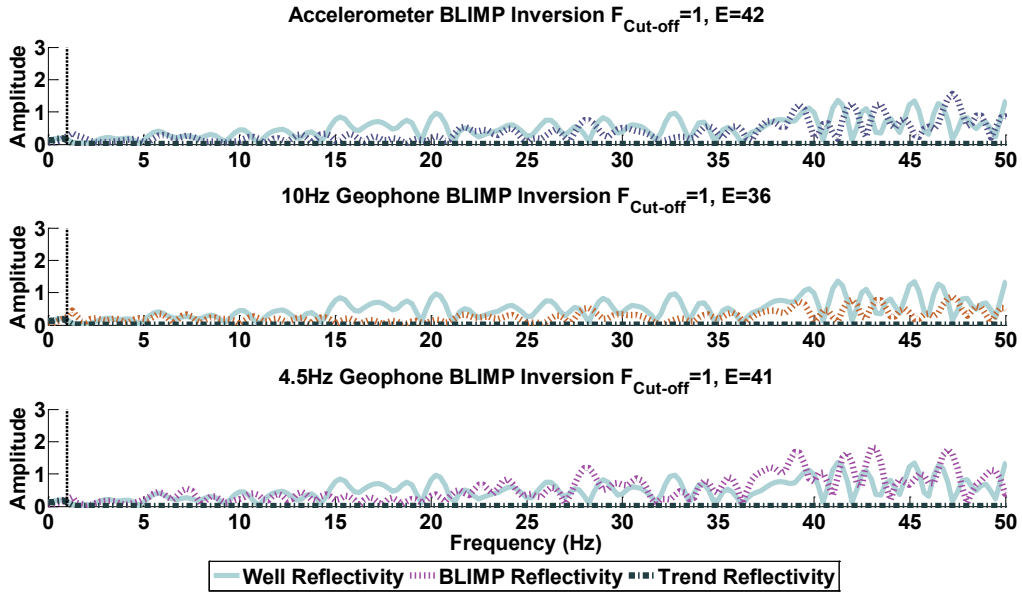

FIG 23: The amplitude spectra of the BLIMP inverted impedance using a low-frequency cut-off of 1Hz. The least squares error (E) was calculated between the well impedance log and the BLIMP inverted impedance.

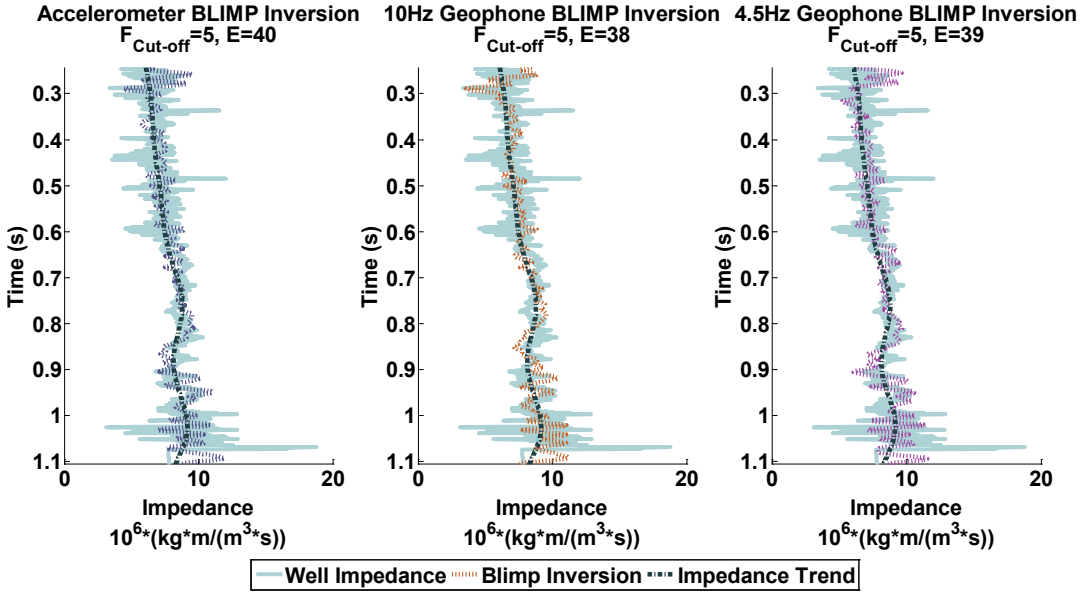

FIG 24: BLIMP inverted impedance using a low-frequency cut-off of 5Hz. The least squares error (E) was calculated between the well impedance log and the BLIMP inverted impedance.

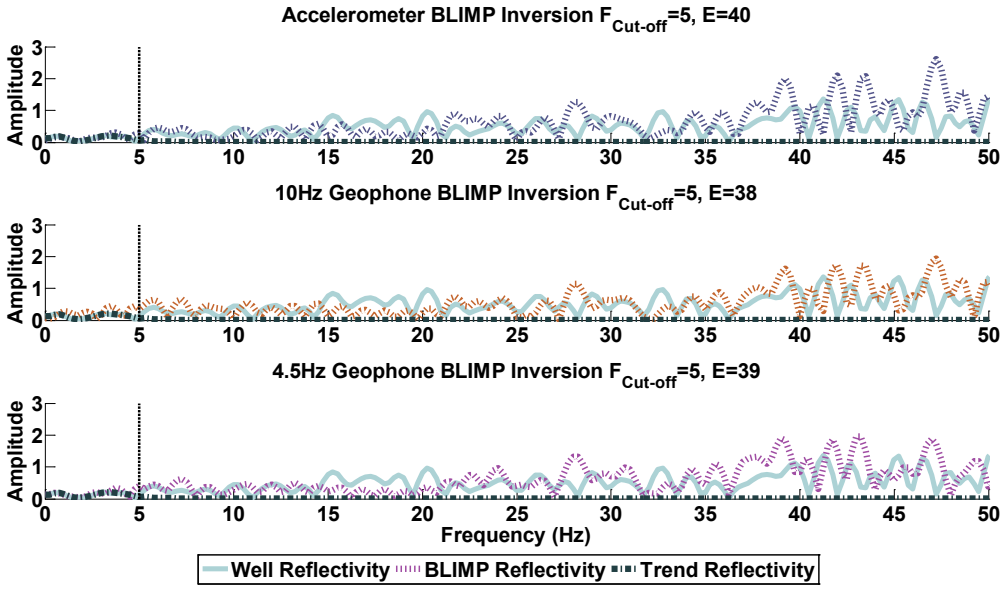

FIG 25: The amplitude spectra of the BLIMP inverted impedance using a low-frequency cut-off of 5Hz. The least squares error (E) was calculated between the well impedance log and the BLIMP inverted impedance.

INOVA Low-Dwell BLIMP Inversion

The BLIMP inversions were also computed on the INOVA low-dwell data. Figure 26 shows the impedance inversion results using a low-frequency cut-off of 1Hz. Unlike the dynamite data these impedance curves do not look similar to one another. Figure 27 shows the amplitude spectra for the impedance inversions. The spectra seem to be similar below 15Hz and look similar again above 25Hz. The spectra also do not appear to match the amplitude spectrum of the well impedance. For the BLIMP inversion using a low-frequency cut-off of 5Hz (Figure 28), the inversions look very similar to one another and to the well. The amplitude spectra of the BLIMP inversions for the 5Hz cut-off are similar to the well spectra and to each other between 25 and 40Hz. The spectra are also similar to each other below 15Hz but do not mimic the well impedance amplitude spectra in this region. Other cut-offs were tested to see how low the low-dwell data could go before the inversions were dissimilar. A cut-off value of 3Hz (Figure 30) was found to produce similar impedance inversions for all of the different receivers.

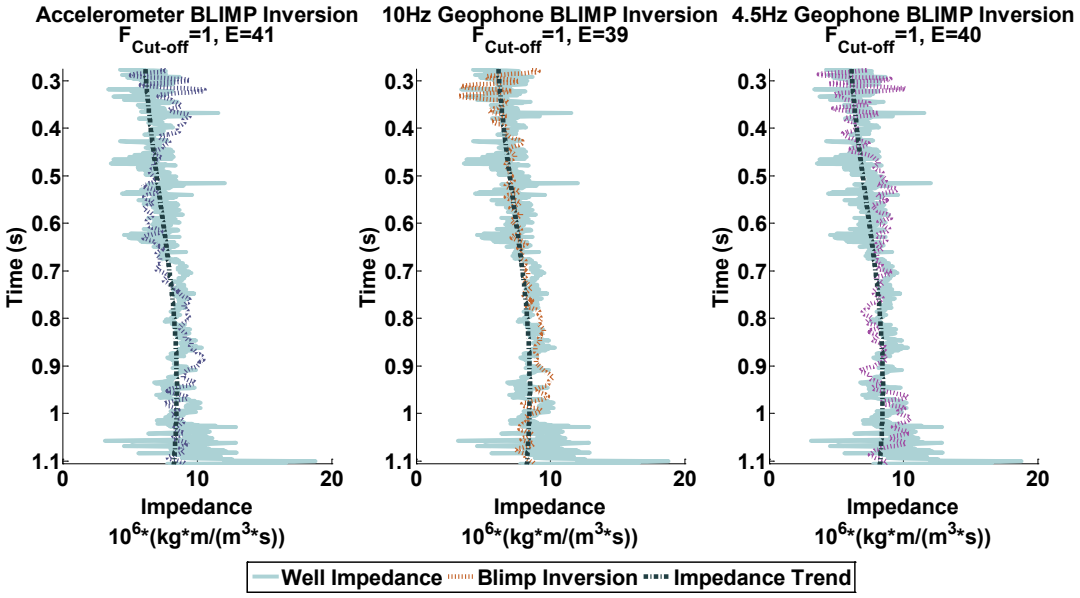

FIG 26: BLIMP inverted impedance using a low-frequency cut-off of 1Hz for the INOVA low-dwell source data. The least squares error (E) was calculated between the well impedance log and the BLIMP inverted impedance.

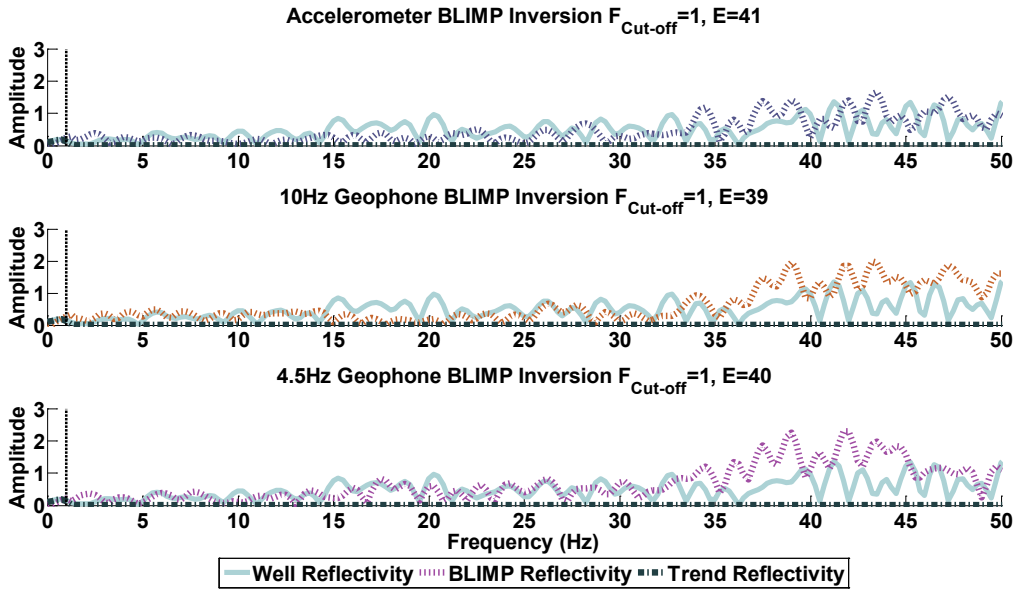

FIG 27: The amplitude spectra of the BLIMP inverted impedance using a low-frequency cut-off of 1Hz for INOVA low-dwell source data. The least squares error (E) was calculated between the well impedance log and the BLIMP inverted impedance.

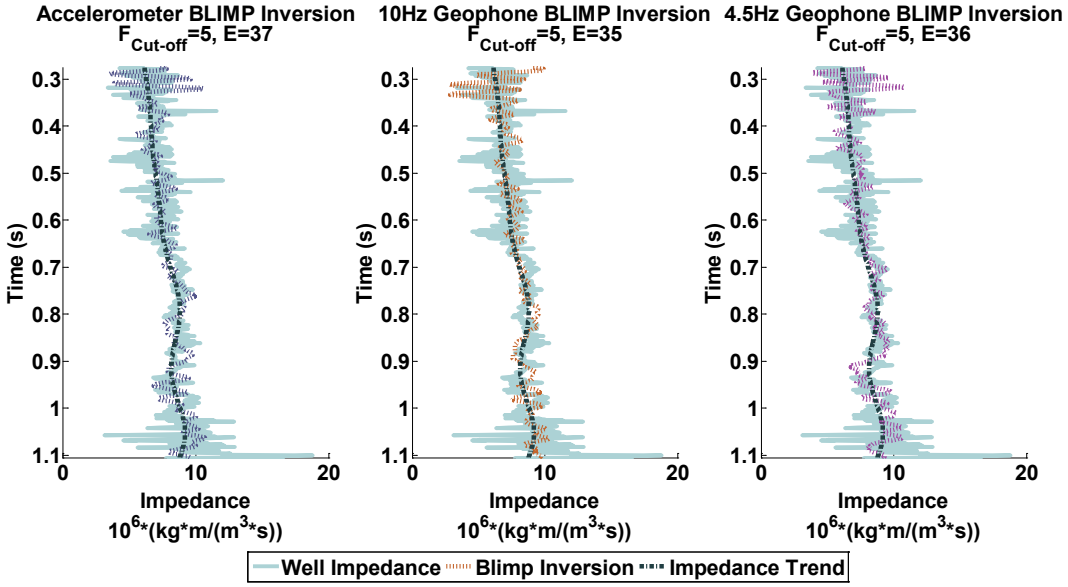

FIG 28: BLIMP inverted impedance using a low-frequency cut-off of 5Hz for the INOVA low-dwell source data. The least squares error (E) was calculated between the well impedance log and the BLIMP inverted impedance.

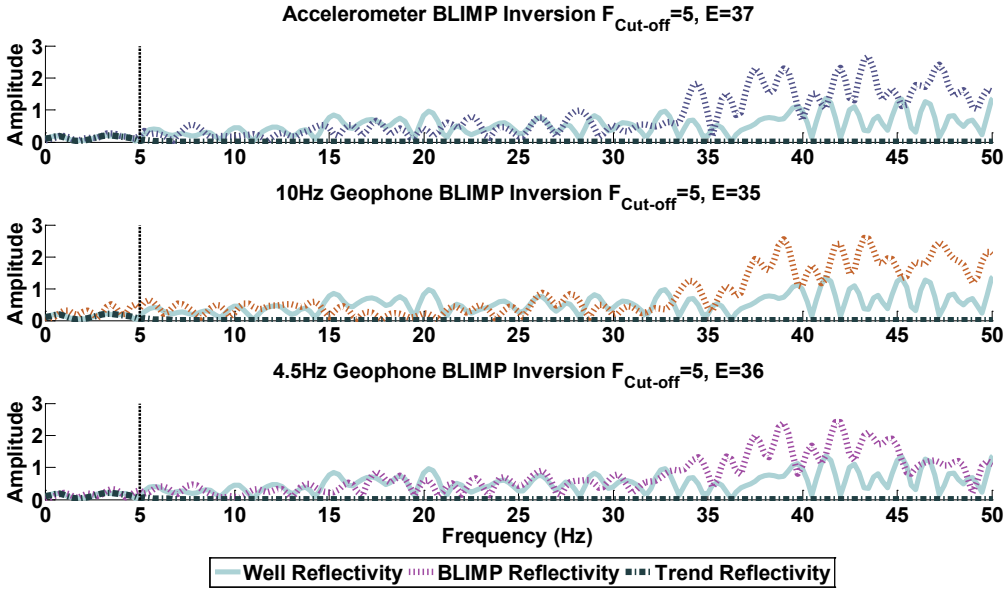

FIG 29: The amplitude spectra of the BLIMP inverted impedance using a low-frequency cut-off of 5Hz, for the INOVA low-dwell source data. The least squares error (E) was calculated between the well impedance log and the BLIMP inverted impedance.

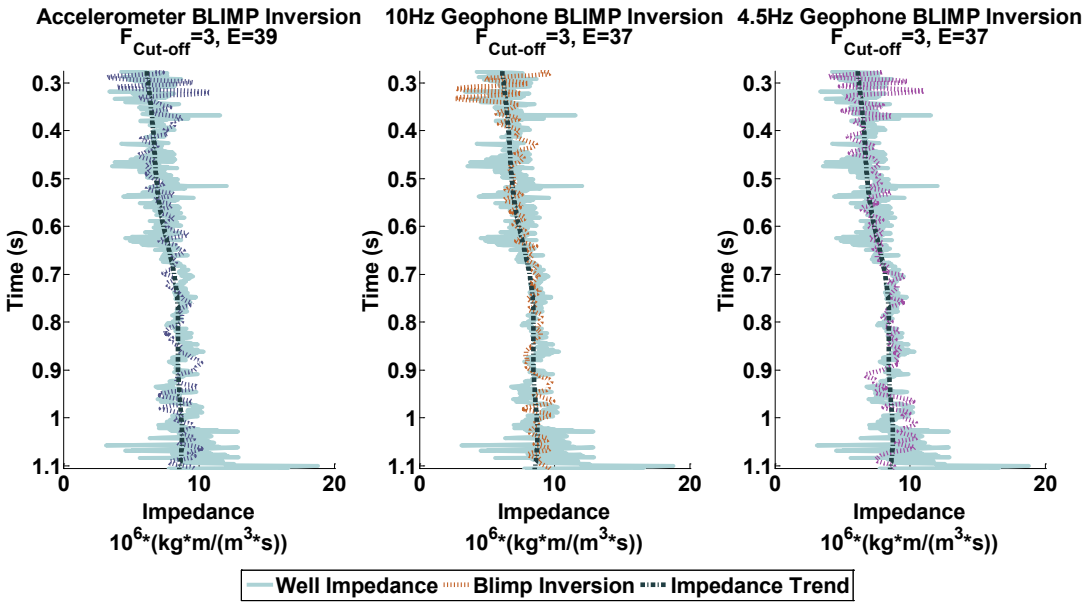

FIG 30: BLIMP inverted impedance using a low-frequency cut-off of 3Hz for the INOVA low-dwell source data. The least squares error (E) was calculated between the well impedance log and the BLIMP inverted impedance.

CONCLUSIONS

To achieve a BLIMP impedance inversion that was similar to the well impedance the low-frequency cut-off needed to be at least 1Hz for the dynamite data and 3Hz for the INOVA low-dwell data. These are promising results as it allows us to complete inversions using very small amounts of well data. When large amounts of well data is used we do not get reliable inversions (Lloyd and Margrave, 2011). This shows that it may be possible to create accurate inversions in non-homogeneous systems and gain accurate information without dominating the signal with well information.

The impedance inversion for the accelerometer and 4.5Hz geophone data had very similar results to one another, suggesting repeatability for the impedance at this location. To fully understand if this was coincidence or not the analysis should be repeated for another well that occurs on the line.

Similar results were found when inverting the INOVA low-dwell data, however a larger low-frequency cut-off of 3Hz, is needed. Vigorous testing and reprocessing must be done to verify the findings in this paper that consistent impedance inversions can be conducted with only using 1Hz of well impedance for the dynamite source and 3Hz of well impedance for the INOVA low-dwell source.

These conclusions must be regarded as preliminary since the data processing is not final, migrated sections were not used, and it is likely that a our well tie can be improved. We also note that the 12-27 well ties the line at the end where fold is low and the data noisy. We plan to study inversions at the two other well ties on the line.

ACKNOWLEDGEMENTS

The authors would like to thank Husky Energy for arranging the site, land access, and licensing, INOVA for providing the INOVA 364 low frequency vibe source, and Geokinetics for providing the seismic crew, recorder and the Vectorseis 3C MEMs accelerometers. The authors would also like to thank Helen Isaac for processing, and reprocessing the Hussar data and Kevin Hall for technical support. Additionally, the authors would like to thank the CREWES sponsors for their continued financial support.

REFERENCES

Ferguson, R. J. and Margrave, G. F., 1996, A simple algorithm for bandlimited impedance inversion: CREWES Research Report, Vol. 8, No. 21.

Isaac, J. H. and Margrave, G. F., 2011, Hurrah for Hussar! Comparisons of stacked data: CREWES Research Report, Vol. 23, No. 55.

Lindseth, R. O., 1979, Synthetic sonic logs – a process for stratigraphic interpretation: Geophysics, Vol. 44, No. 1.

Lloyd, H. J. E. and Margrave, G. F., 2011 Bandlimited impedance inversion: using well logs to fill low-frequency information in a non-homogenous model: CREWES Research Report, Vol. 23, No. 71.

Margrave, G. F., Mewhort, L., Phillips, T., Hall, M., Bertram, M. B., Lawton, D. C., Innanen, K. A. H., Hall, K. W. And Bertram, K. L., 2011, The Hussar Low-Frequency Experiment: CREWES Research Report, Vol. 23, No. 78.

Oldenburg, D. W., Scheuer, T., and Levy, S., 1983, Recovery of the acoustic impedance from reflection seismograms: Geophysics, Vol. 48, No. 10.